

Retrieval theoretical basis of NICT/SMILES level-2 products:

upper tropospheric cloud ice mass and water vapor

Authors: Yasko Kasai (1)

Bengt Rydberg (2)

Joakim Möller (2)

(1) National Institute of Information and Communications Technology

(2) Molfrow

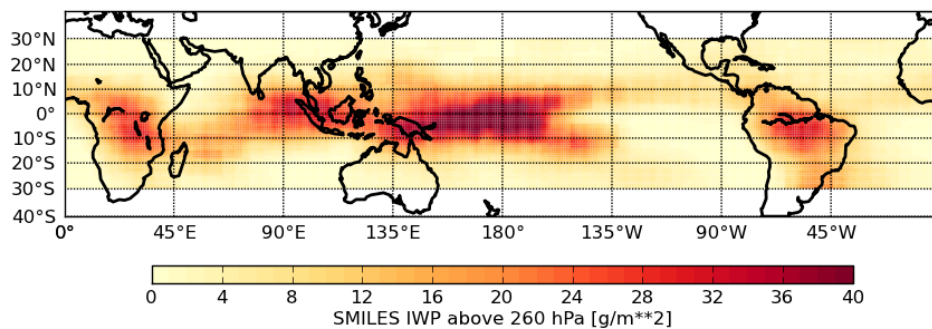
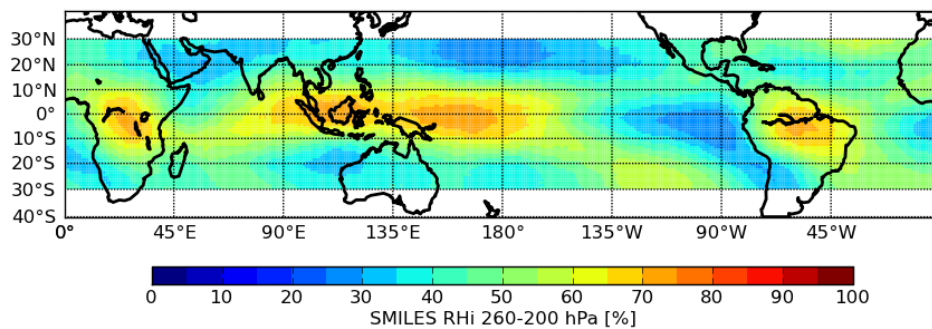
Version: 1.0

Date: 2014-04-29

Contact: For additional details on these products, please contact the NICT/SMILES developing team <smiles-data-access@ml.nict.go.jp>. PI and 1st contact person: Yasko Kasai.

Abstract

The sub-millimeter-wave limb-sounder (SMILES) on-board the International Space Station (ISS) operated from 2009-10-12 until 2010-04-21, and provided observations of cloud ice and water vapor in the uppermost tropical troposphere. This document describes new SMILES level2 products: column ice mass above 260 hPa and humidity between 260-200 hPa.



Contents

1 Introduction	2
1.1 Overview	2
1.2 Scientific interest	3
2 SMILES	3
2.1 Overview	3
2.2 Observations considered	3
3 Retrieval approach	4
3.1 Retrieval theoretical basis	4
3.2 Retrieval database	4
3.2.1 Atmospheric states	4
3.2.2 SMILES measurement simulations	4
3.2.3 Comparison of SMILES measurement with simulations	5
3.3 Retrieval procedure and setup	9
3.4 Retrieval characterization	10
3.4.1 Cloud ice	10
3.4.2 Humidity	14
4 The level2 products	17
4.1 The IWPRH product	18
4.2 The H2O product	19
4.3 Data quality and filtering recommendation	19
4.4 Example results	21

1 Introduction

1.1 Overview

The Superconducting Submillimeter-Wave Limb-Emission Sounder (SMILES), carried by the International Space Station (ISS) collected atmospheric emissions around 625 and 650 GHz from 2009-10-12 until 2010-04-21. The limb scanning was performed from altitudes below the surface up to around 100 km. Measurements from the lowest part of the scan has sensitivity to water in the upper troposphere. This report describes new SMILES level2 products of tropical upper tropospheric cloud ice mass and relative humidity derived from these measurements.

The report has the following contents:

the SMILES observations considered is described in Section [SMILES](#),

the retrieval technique, and how it was applied for SMILES observations, is described in Section [Retrieval approach](#),

Section [Retrieval characterization](#) contains an error characterization of the retrieval parameters,

The level2 products (e.g. the file-format) are described in Section [The level2 products](#).

1.2 Scientific interest

The circulation of water through the atmosphere is highly important for the Earth's climate system, but it is not fully understood. Water exists in the form of water vapor and cloud ice particles, in the uppermost part of the troposphere in the tropical region. Ice clouds and water vapor, in this particular part of the atmosphere, have a strong impact on, for the climate so important, the fluxes of incoming solar radiation and outgoing long wave radiation. The occurrence of ice clouds are influenced by the solar diurnal variation, and ice clouds have therefore also a diurnal variation.

SMILES not only provides observations of cloud ice and water vapor in the uppermost tropical troposphere. The orbit of ISS gives also that the average diurnal variation of cloud ice and water vapor can be derived from SMILES observations. These observations are therefore of interest in the area of climate research.

2 SMILES

2.1 Overview

The Superconducting Submillimeter-Wave Limb-Emission Sounder (SMILES), carried by the International Space Station (ISS), collected atmospheric emissions around 625 and 650 GHz from 2009-10-12 until 2010-04-21. SMILES was developed by National Institute of Information and Communications Technology (NICT) and Japan Aerospace Exploration Agency (JAXA). The main scientific objective of SMILES was to measure, with a high precision, middle atmospheric minor constituents, such as O₃ (including isotopologues), HCl, ClO, HO₂, BrO, and HNO₃, and to determine the diurnal change of these species. It was also known pre-launch that SMILES had sensitivity to upper tropospheric humidity and ice clouds, but the instrument was not optimized for this purpose. Kikuchi¹ et al. (2010) provides an overview of the SMILES mission, Ochiai⁴ et al. (2012) gives an overview of the calibration of SMILES, and standard level 2 products are described by Takahashi et al. (2010) and Baron et al. (2011).

The inclination of the ISS orbit is 51.6 degree to the equator, and ISS had an altitude between 333 and 370 km during the SMILES operation. SMILES measurements cover latitudes between approximately 38 degree S to 65 degree N. An unique characteristic of SMILES' measurement coverage is the local time variation. The local time of observations for a given region shifts by 24 hour per 60 days.

SMILES could measure in three 1.2 GHz wide frequency bands: 624.32 - 625.52 (Band A), 625.12 - 626.32 (Band B), and 649.12 - 650.32 GHz (Band C), but only two of them were measured simultaneously, with two acousto-optical spectrometers. Band combinations were altered on a time-share basis.

The receiver noise temperature was about 350 K. The size of the antenna beam, at the tangent point, was about 3 and 6 km in the vertical and horizontal direction, respectively. The scanning was performed from altitudes below the surface up to around 100 km, at an angle of about 45 degree from the orbital plane and with a repetition period of 53 s (~1630 scans/day).

2.2 Observations considered

The retrievals presented here only use single spectra from the tangent heights between -30 and 8 km within 30 degree S to 30 degree N. For those measurements the atmosphere below ~10 km is opaque, and this reduces the complexity of the retrieval. The observation geometry can be seen as slant down-looking (see Figure 1).

One "window" channel, from each of the two band that is measured simultaneous, centered around 624.61(A), 626.23(B), and 649.61(C) GHz and with a bandwidth of 10 MHz, are used in the retrieval. The latter band (C) "sees" roughly 500 m further down in the atmosphere than the two others. The "best" measurement will therefore be obtained when band C is measured together with any of the two others. The horizontal footprint size at 10 km altitude is in the order of 40 x 7 km² for measurements in the tangent-height range used.

Used SMILES L1b data are of calibration version 008. In this version, the determination of both brightness temperatures and tangent heights has been improved compared to earlier versions (Ochiai ⁴ et al., 2012). The tangent height accuracy is now about 140 m, but occasionally the errors can be larger than 200 m. The largest error source in the intensity calibration scheme is the gain non-linearity (~1 K), which is well above the thermal noise level, which is ≈ 0.15 K for the frequency bands selected.

3 Retrieval approach

3.1 Retrieval theoretical basis

The retrieval technique applied for SMILES observations is described in Rydberg ² and was developed and successfully applied to similar measurements from the sub-millimeter-radiometer (SMR) on board the Odin satellite. This retrieval technique is a Bayesian Monte Carlo integration method where Bayes theorem is used to retrieve the conditional expected value of the atmospheric state for a given measurement. The retrieval technique takes into account that the retrieval problem is non-unique and non-linear, and that upper tropospheric water exhibits non-Gaussian statistics.

The retrieval technique is based on a "retrieval database", consisting of atmospheric states and simulated measurements. The atmospheric states in the retrieval database should ideally have the same statistical distribution as in reality. The retrieval algorithm effectively "interpolates" between the states that approximately match a given measurement. The retrieval algorithm also provides an error estimate.

3.2 Retrieval database

3.2.1 Atmospheric states

When this technique was applied to Odin-SMR observations an atmospheric data set consisting of ~12000 atmospheric states for tropical conditions was created. Sources to this data set is the Cloud Profiling Radar (CPR) on board CloudSat, ECMWF data, and climatology data. The states have a 3-dimensional variability and consist of fields of temperature, humidity, ice water content, and trace gases. Ice water content [g/m^3] is the concentration of cloud ice mass. The cloud micro physics, here particle size distribution (PSD) and shapes, of ice particles are complicated to represent due to a combination of its complexity and natural variability and lack of knowledge. In this data-set it is assumed that the PSD follows a parameterization ⁶ derived from measurements from tropical conditions. It is further assumed that solid ice spherical particles is a fair representation when the target is sub-millimeter observations of cloud ice mass. The retrieval errors due to these simplifications are discussed in Retrieval characterization.

In each state the "cloud-box" region, i.e. the region where cloud particles can exist, has a limited size (4 degree in latitudinal extension, see figure below). This atmospheric data set is reused for SMILES. The aim is therefore to simulate accurate SMILES measurements for these ~12000 atmospheric states, for the tangent height range and frequencies considered.

3.2.2 SMILES measurement simulations

SMILES measurement simulations are performed using the atmospheric radiative transfer simulator (ARTS ⁵ [v.2.1.406]). We only simulate radiance for 1 frequency per band: 624.61 (A), 626.23 (B), and 649.61 (C) GHz. For each state we only simulate measurements for the lowest tangent altitude range of SMILES [-30 km:200m:8 km]. Gas species included in the calculations are H₂O, N₂, N₂O, O₂, O₃, ClO, and HNO₃.

Important spectroscopy settings are:

N₂ absorption follows Liebe et al. (1993) and this absorption is scaled with a factor of 1.34 as suggested by Boissoles et al. (2003),

The water vapor "continuum" parametrization follows Podobedov et al. (2008),

The measurement simulations performed can be divided into three steps:

step1: For each atmospheric state, we simulate clear sky radiative transfer for a number of pencil beams from a fixed (see figure below) sensor position and extract state parameters along the pencil beams (state parameter: ice water, relative humidity, and temperature)

step2: For those pencil beams that were "contaminated" with cloud particles, we repeat the simulations, but now using the Monte Carlo module of ARTS that handle scattering. The Monte Carlo precision is set to 1 K for each pencil beam.

step3: Instrument response calculation. We perform an antenna weighting of the pencil beam radiance's and state parameters. The obtained simulated measurements and 1-dimensional antenna weighted state parameters will be the actual input to the retrieval calculation.

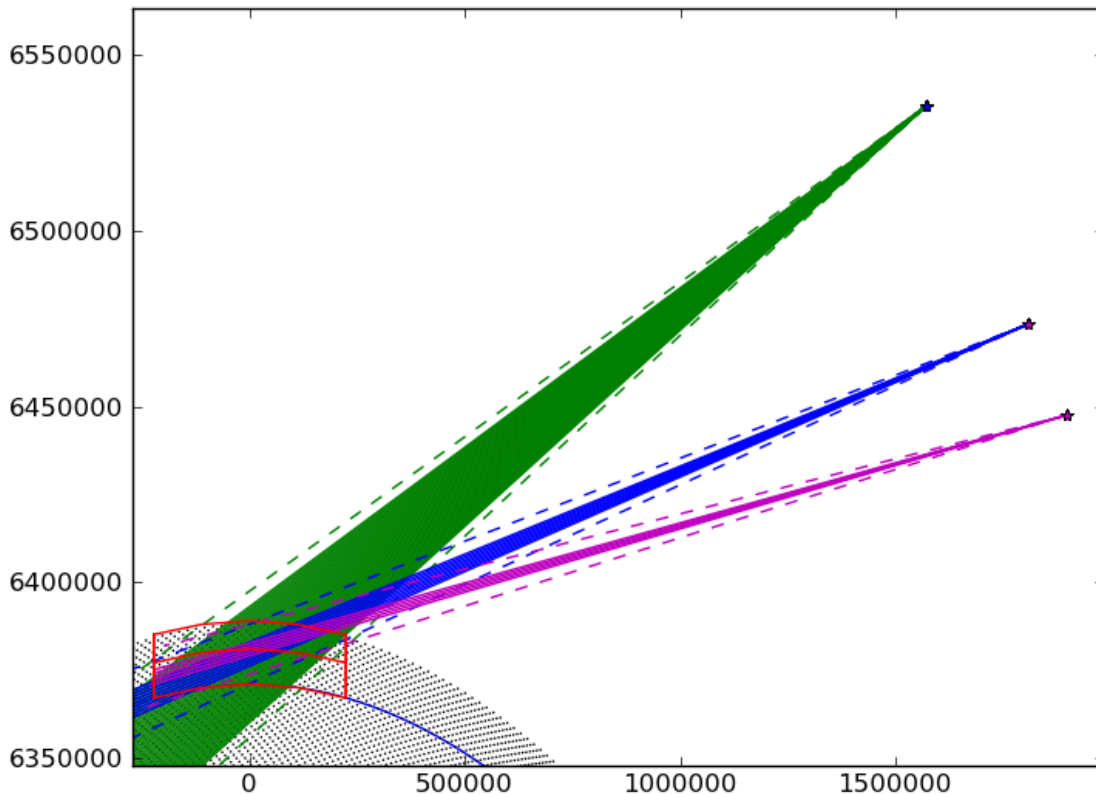


Figure 1. Observation geometry for the three different setups that cover different tangent-height ranges (green: -30- -4 km, blue: -4- 4 km, magenta: 4- 8 km. SMILES are placed at three different locations (the stars in the figure) at an altitude of 350 km. The red area are the "cloud-box" region described in text (4 degree latitudinal extension and the vertical lines are placed at 0, 9, and 18 km in altitude).

3.2.3 Comparison of SMILES measurement with simulations

One way to "validate" the retrieval database is to compare it to real measurements. The variability and distribution of atmospheric states in the retrieval database were created to match with the reality. Hence, the distribution of simulated measurements should agree with real SMILES measurements. This comparison is sensitive to both the spectroscopic setup of the simulations and to the intensity calibration of SMILES.

Figure 2 shows a simple comparison of distributions of real and simulated SMILES measurements for Band-A, Band-B, and Band-C. Only measurements with brightness temperatures above 190 K are displayed. That is, these measurements are either from clear sky or close to clear sky conditions. Both the peaks and widths of the distributions for the measurements and simulations for all Bands show a reasonable agreement, although the spread in the distributions is wider for the simulations than for the

measurements.

In Figure 3 the differences are examined further. Figure 3 shows how the distribution (visualized as percentiles) of T_b vary as function of tangent altitude for real SMILES measurements and simulations. For example, the 50%-percentile (median) shows that 50% of the data-points are below this limit. Figure 3 also shows that the distributions are wider for the simulations than for the measurements. The differences are less than 1 K for most data-points of the percentiles, and the agreement is judged to be high.

Figure 3 shows also that the difference in T_b , for observations with -30 km and 8 km tangent points, is around 5 K (for the 50%-percentiles). The measurements and simulations agree almost perfectly with respect to this point.

The agreement seen in Figure 2 and 3 is such that we conclude that the accuracy of the clear sky simulations is better than 1 K with respect to calibrated SMILES measurements. The consequence for the accuracy of the retrieval parameters is discussed in Section [Retrieval characterization](#).

We now continue with a qualitative comparison of measurements and simulations effected by cloud scattering. Figure 4 shows a basic comparison of the 2-dimensional probability distributions of SMILES and simulated measurements for band A and C. Clear-sky cases are located in the top right corner (T_b above ~ 195 K), and cloudy cases in the lower left part. The two distributions shows a high degree of agreement. This is not a proof, but an indication that the simulations are handled realistically. Figure 5 shows similar data as Figure 4 but for band A and B. The agreement between measurements and simulations are also good for this band combination. Figure 5 shows also that band A and B measurements contain less independent information for these observations than band A and C, as the data points are close to a one to one line.

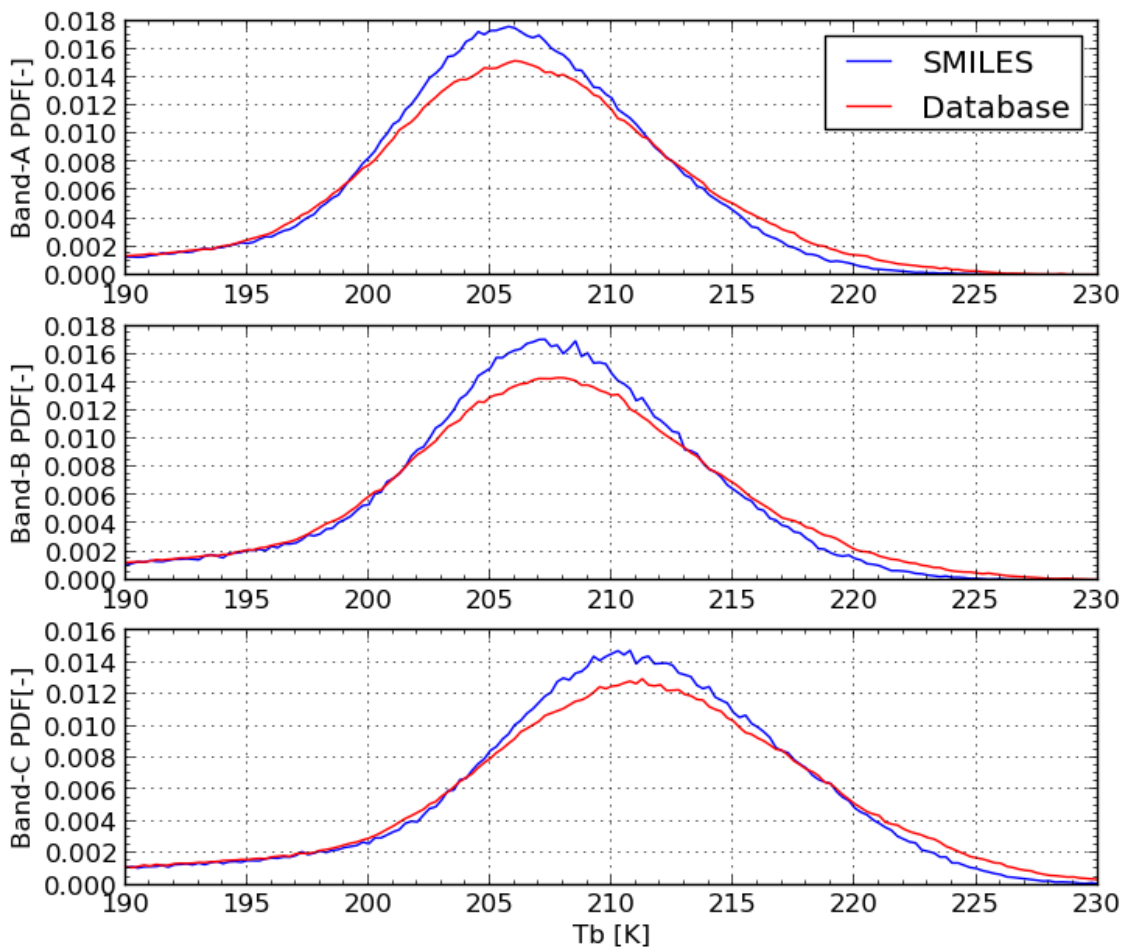


Figure 2. Probability density functions (PDFs) of simulated (red) and real (blue) SMILES measurements for tangent heights between -30 to 8 km in the tropical region. The simulations were performed for the atmospheric states in the retrieval database. The upper panel shows data from Band-A, the middle panel Band-B, and the lower panel Band-C.

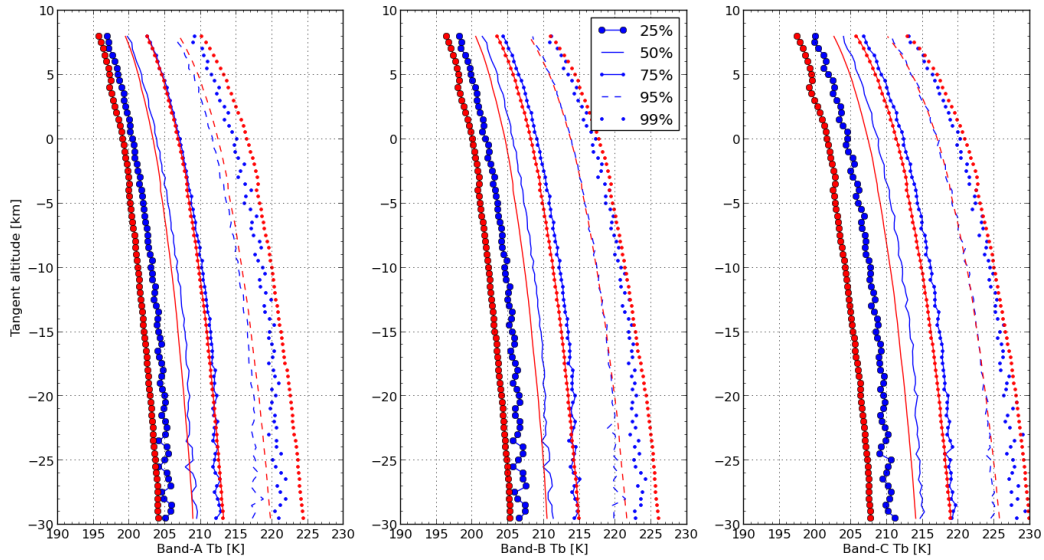


Figure 3. Distribution of Tb as function of tangent altitude for SMILES measurements and simulations within the tropical region. The panels show data for 25%, 50%, 75% , 95%, and 99% - percentiles for Band-A (left panel), Band-B (middle panel), and Band-C (right panel). Blue and red lines represent real and simulated SMILES measurements, respectively.

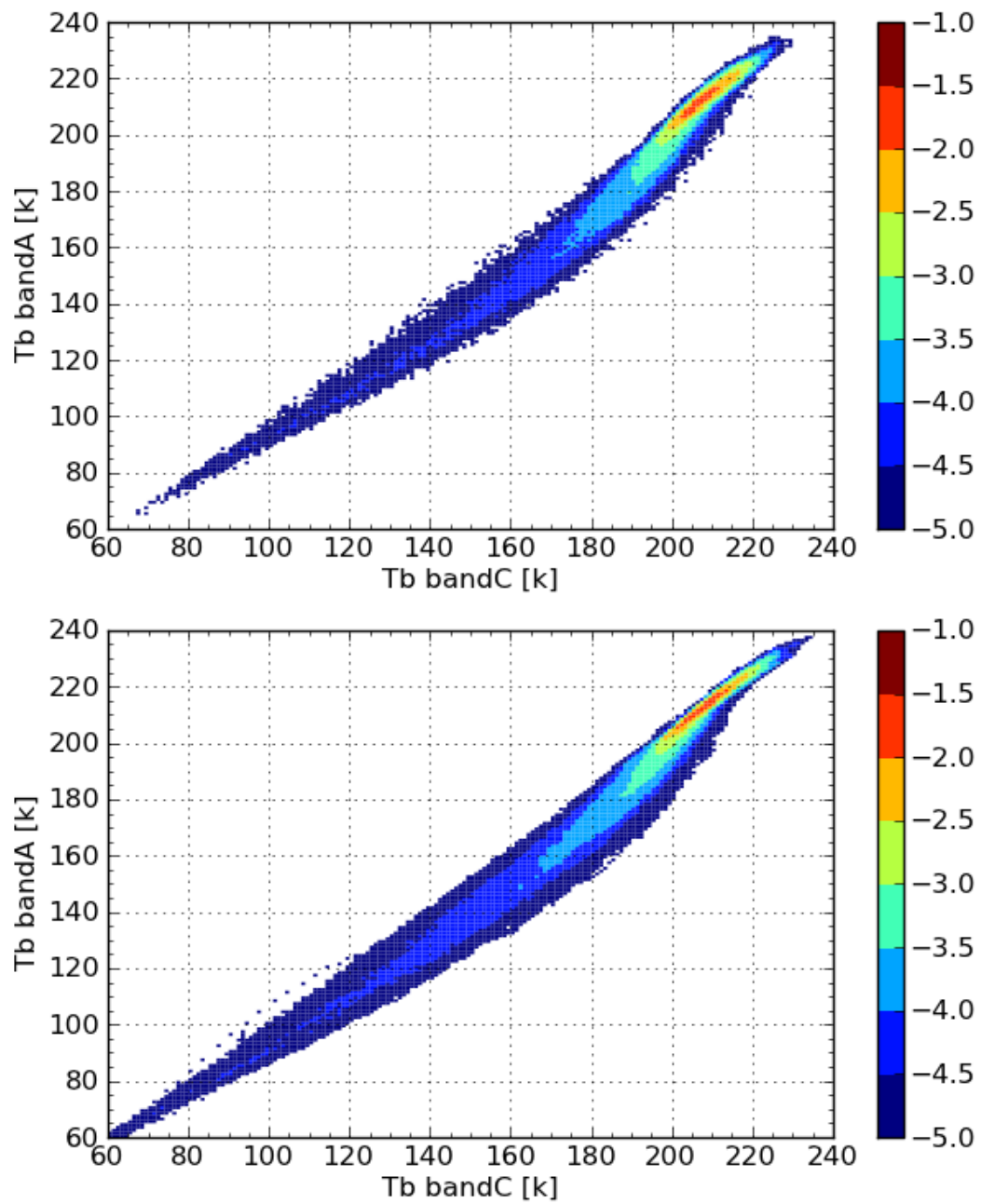


Figure 4. Probability distribution of SMILES measurements (upper panel) and simulations (lower panel) for band C and A for tangent heights between -30 to 8 km in the tropical region. The color-coding represents the logarithm of the probability.

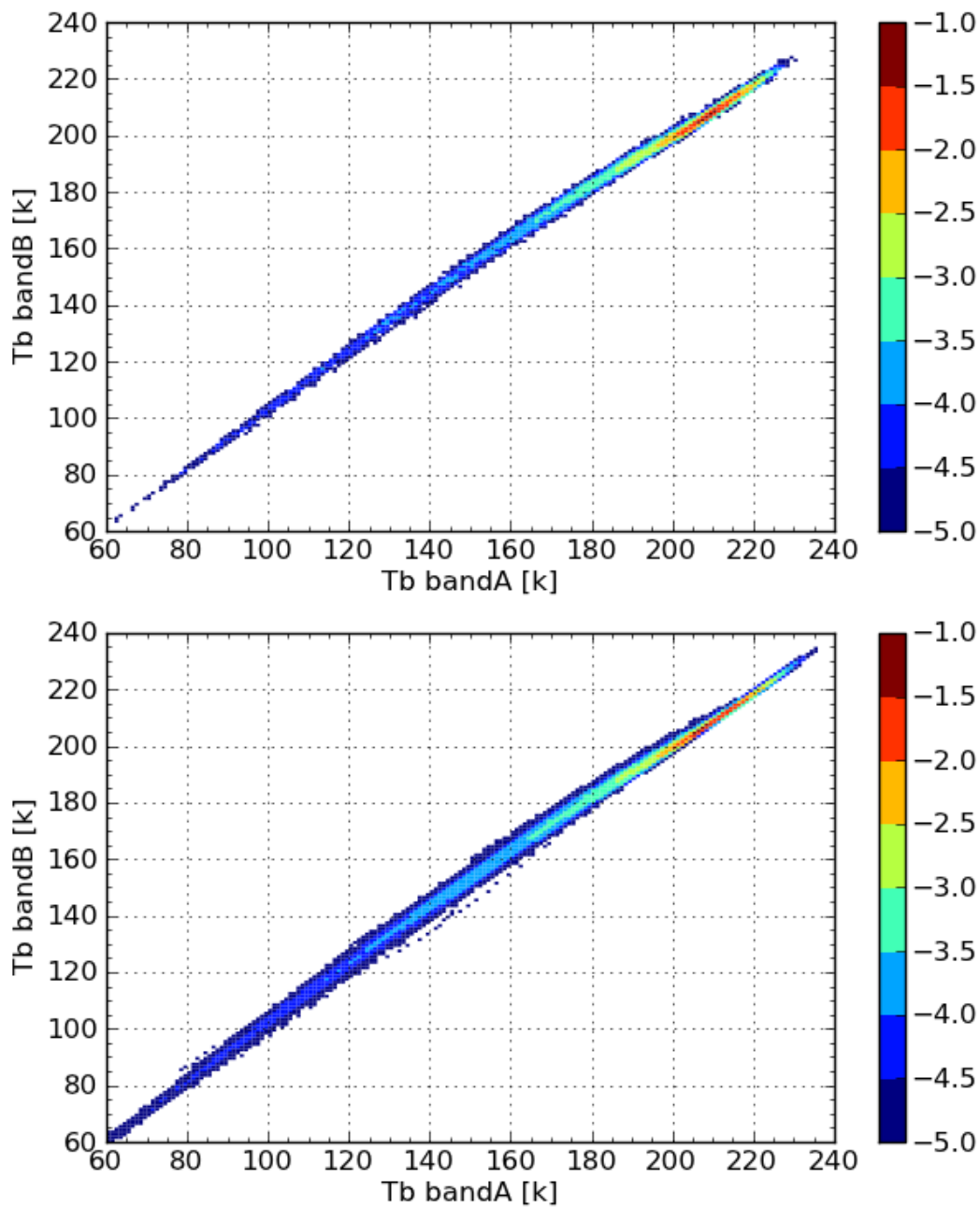


Figure 5. Same as Figure 4 but for bands A and B.

3.3 Retrieval procedure and setup

The retrieval methodology described in [Rydberg² et al.,2009](#) is applied. The retrieval procedure for its application to SMILES-data is here outlined:

1. Level1b-reading: extract window averaged brightness temperature (Tb) from the two measured bands, system noise temperature, the tangent-height, and the antenna rotation angle, latitude and longitude of tangent point, and the antenna orientation from SMILES level1b-data.

2. Geo-location estimation: The point where the line of sight between SMILES and the tangent point is 10 km above the surface is estimated and taken as a measure of the geo-location of each sounding.
3. Extract ECMWF temperature information from the position estimated above.
4. Retrieval calculation: Treat the following four elements:

Average Tbs from the two measured bands; Band A 624.61 GHz +-5MHz, Band B 626.23 GHz +-5MHz, Band C 649.61 GHz +-5MHz The tangent-height

ECMWF temperature at 200 hPa

as the measurement vector. The retrieval requires the setup of an error covariance matrix, in this case a matrix of size 4x4. The elements of the diagonal of this matrix describes the uncertainty of the elements of the measurement vector. All off-diagonal elements are set to 0. The 1-sigma uncertainties used are listed below.

The Tb uncertainty (1-sigma) is determined from the intensity calibration uncertainty of ~1 K (due to gain non-linearity, [Ochiai⁴](#) et al., 2012) and thermal noise (~0.15 K; $T_{sys} \sim 320$, $T_{int} \sim 0.5$ sec., $B = 10$ MHz), which together gives an uncertainty of ~ 1.01 K ($\sqrt{1^2 + 0.15^2}$).

The tangent-height uncertainty (1-sigma) is set 200 m (accuracy is 140 m and precision is 50 m, ([Ochiai⁴](#) at al., 2012))

The ECMWF temperature uncertainty is set to 1 K.

Inverse calculation: the retrieved parameters are a weighted average of of the atmospheric states in the retrieval database, where the weight for each state depends on the match between the SMILES measurement vector and the simulated measurement vector, taking into account of the uncertainty (the measurement error covariance matrix).

3.4 Retrieval characterization

Retrieval simulations were performed to characterize the retrieval and to find the most suitable retrieval parameters. The retrieval simulations were done by inverting simulated measurements from the retrieval database where the true atmospheric states are known.

3.4.1 Cloud ice

The retrieval methodology allows for retrievals on an arbitrarily fine grid, due to the a priori usage. However, our aim is to limit the a priori influence of the retrieval as much as possible. The basic measurement information comes from only two channels, and for the combination of Band-A and Band-B measurements the two channels are not very independent. Thus, it seems reasonable to aim for retrieval in one or two layers.

Figure 6 shows retrieved ice water content (IWC) for four vertical layers. Below 250 hPa the retrieval precision is significantly lower than for the two closest layer above. The reason for this is basically that the measurements have little sensitivity to IWC in the lowermost layer. The retrieval precision for the layer between 150-100 hPa is worse than the two layers below. The retrieval also tends to underestimate IWC for this layer. The reason for this is most likely due to limited vertical resolution of the measurements. The retrieval seems to place IWC at this layer in one of the layer below, as this is more likely according to the a priori.

The precision is around 50 % for IWC values above 1 mg/m³, for the layers above 250 hPa. The vertical resolution was concluded to be coarse for these "down-looking" measurements, and from Figure 6 it was judged that a suitable cloud ice mass retrieval parameter would be the ice water path (column integrated ice water content) above around 250 hPa (260 hPa was finally selected). Figure 7 shows that the retrieval precision is in the order of 50 % for IWP values above 1 g/m².

Figure 7 shows also that the retrieval precision is best for IWP values between a few mg/m² to around 100 mg/m². The reason for this is examined in Figure 8, which shows statistics of the relationship between simulated Tb and IWP for the states in the retrieval database. Figure 8 shows that for IWP values of a few mg/m² simulated TB is well below possible humid clear sky values. Figure 8 shows also that the

spread between IWP and Tb for IWP values in the range of 10- 70 g/m² is much smaller than for IWP values above 100 g/m². Furthermore, Figure 8 shows that above 100 mg/m² there is a clear deviation between median values of Tb as function of IWP and median values of IWP as function of Tb. The consequence of this is discussed below.

Figure 8 shows that if we were to perform a large number of measurements for states with pIWP values around 1000 g/m², the median value of Tb would be around 90 K. The relationship between median values of IWP as function of Tb can thought of as a simplified retrieval algorithm using a priori information. For example, given a Tb of 90 K, the retrieved IWP value would then be around 700 g/m², and for a single measurement this estimate would represent a best guess. But on average this would lead to an underestimation by 30%. How such a priori influences on average data can be taken into account is discussed in [Rydberg²](#).

The estimated random error (from Figure 7) includes effects of thermal noise, uncertainties due to instrument gain non-linearity, pointing error, uncertainty in atmospheric temperatures, cloud inhomogeneities, and smoothing error. There are also other error sources not covered by these simulations that will add to the uncertainty. The full natural variability of cloud micro-physics, i.e deviations from the assumed particle size distribution (PSD), and variations in particle shapes or single scattering properties (SSP), are not captured by the retrieval database. It is also likely that cloud inhomogeneities effects are not fully captured by the simulations. In Table 1 estimates of these error sources are given. The uncertainties due to cloud micro-physics variation derived for similar Odin-SMR observations (see [Eriksson³](#)) are directly translated to these SMILES observation. In Table 1 also the effect of a 1 K calibration error for an intermediate thick cloud is displayed. This is mainly included to give an indication on that any unforeseen errors that have a limited impact on Tb are small compared to other uncertainties.

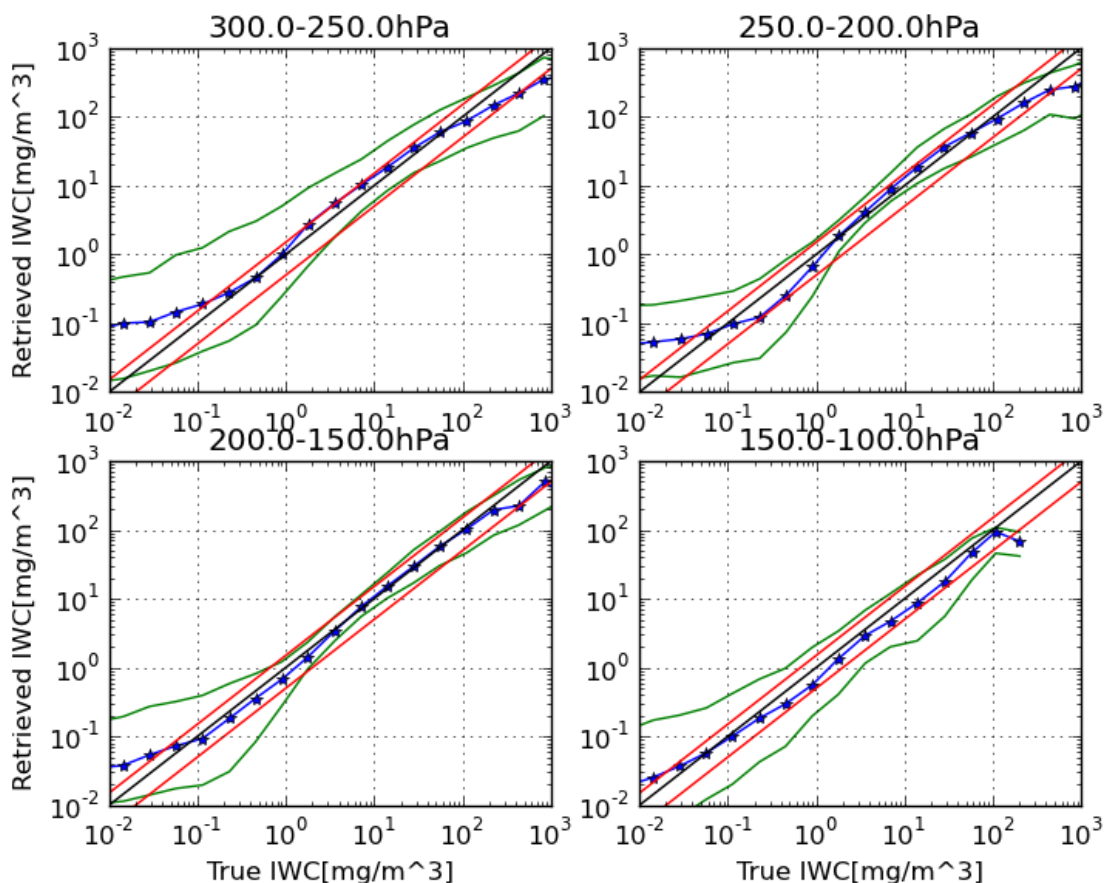


Figure 6. Statistics of simulated ice water content retrieval for four different vertical layers from band A and C measurements. Blue lines show median values, green lines 16 and 84% percentiles, black lines are one to one lines, and red lines represent a 50% error.

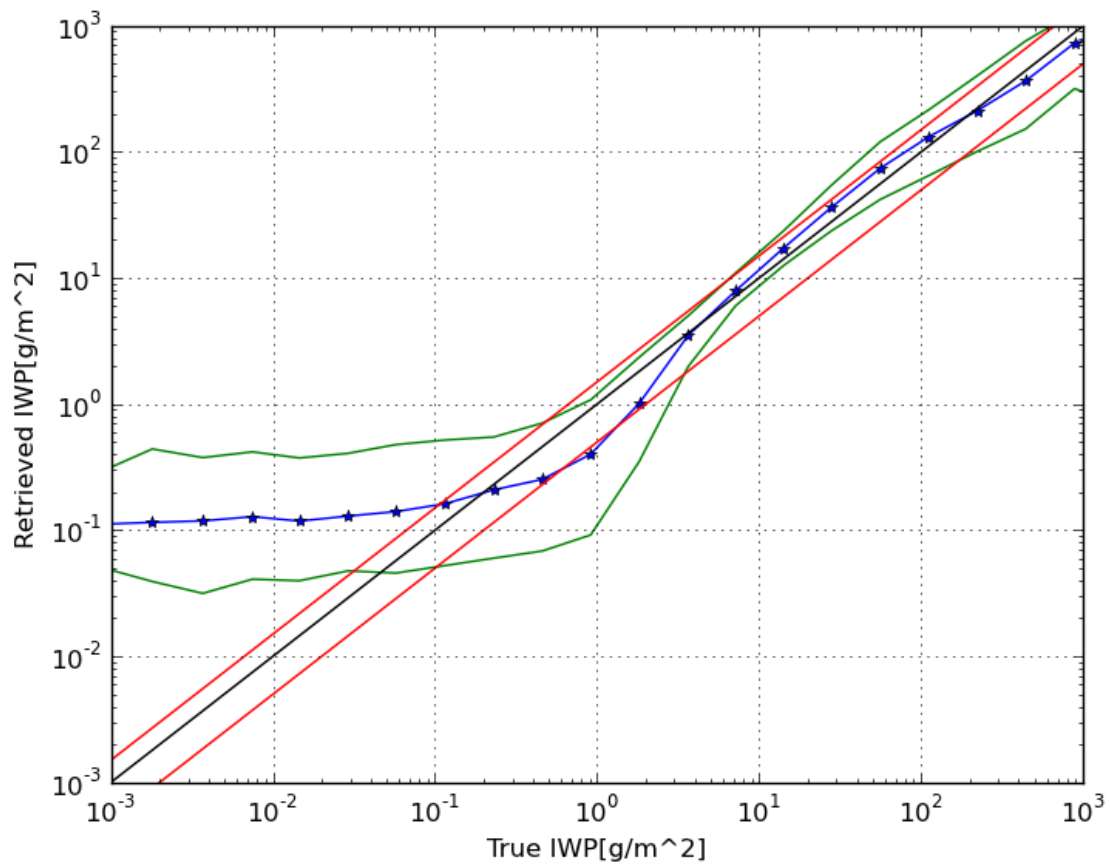


Figure 7. As Figure 6 but for ice water path above 260 hPa.

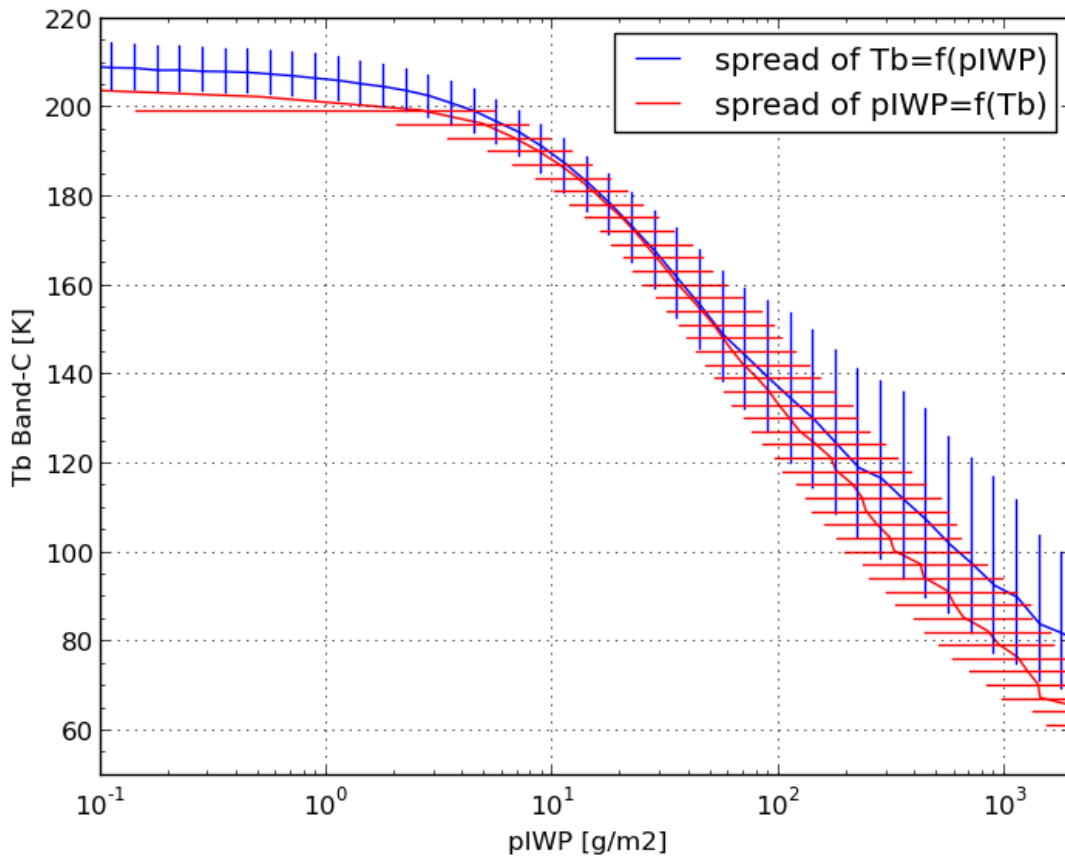


Figure 8. Statistics of simulated Tb for Band-C vs. ice water path above 260 hPa for the states in the retrieval database. The blue line shows the median values of Tb as function of pIWP. The blue error-bars are 16%- and 84%-percentiles and represent a +-1 sigma spread. The red lines show pIWP as function of Tb in an analogous manner.

Table 1. Estimated error from various sources for the ice cloud product.

Error source	perturbation	dTb	error
Systematic errors			
Cloud inhomogeneity	•	•	15%
PSD	•	•	30%
SSP	•	•	15%
Root Sum Square , Systematic errors			37%
Random errors			
Captured uncertainty	•	•	50%
Cloud inhomogeneity	•	•	20%
PSD	•	•	40%
SSP	•	•	15%

Calibration, Tb	1 K	1 K	5%
Root Sum Square , Random errors			69%

3.4.2 Humidity

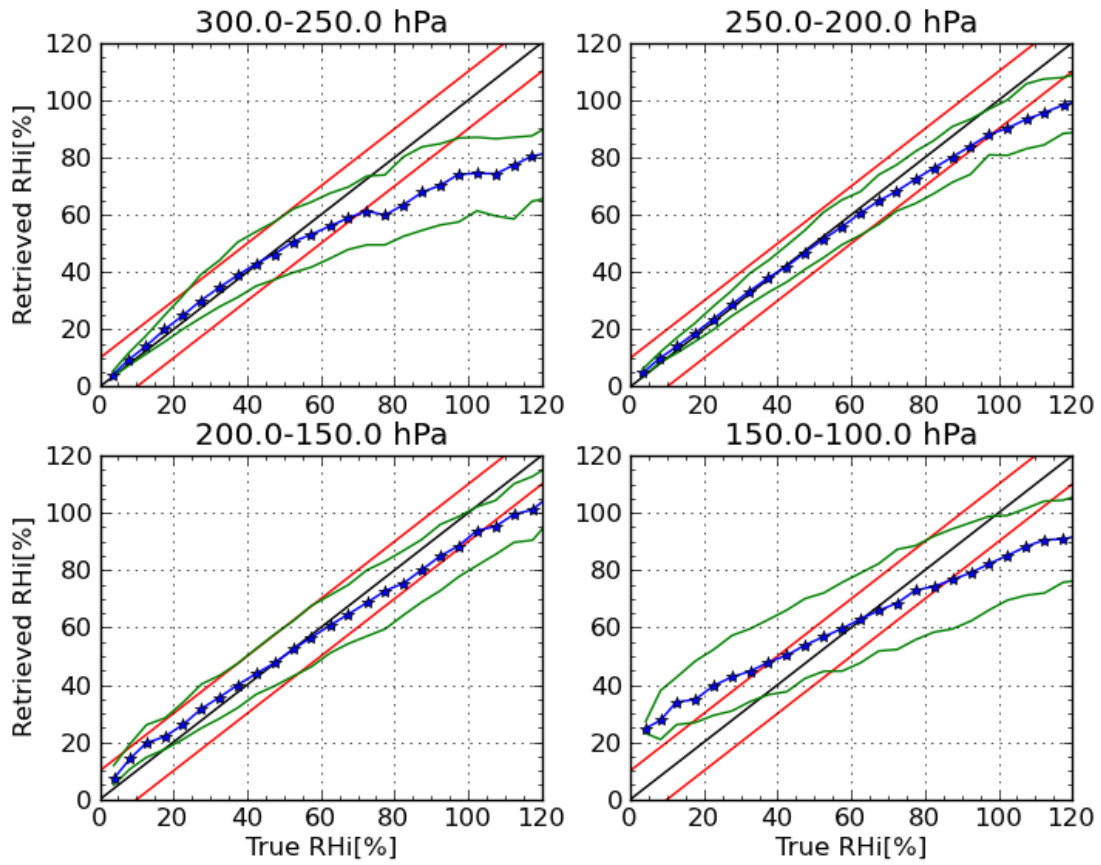


Figure 9. As Figure 6 but for relative humidity w.r.t. ice, and red lines represents a 10 % error.

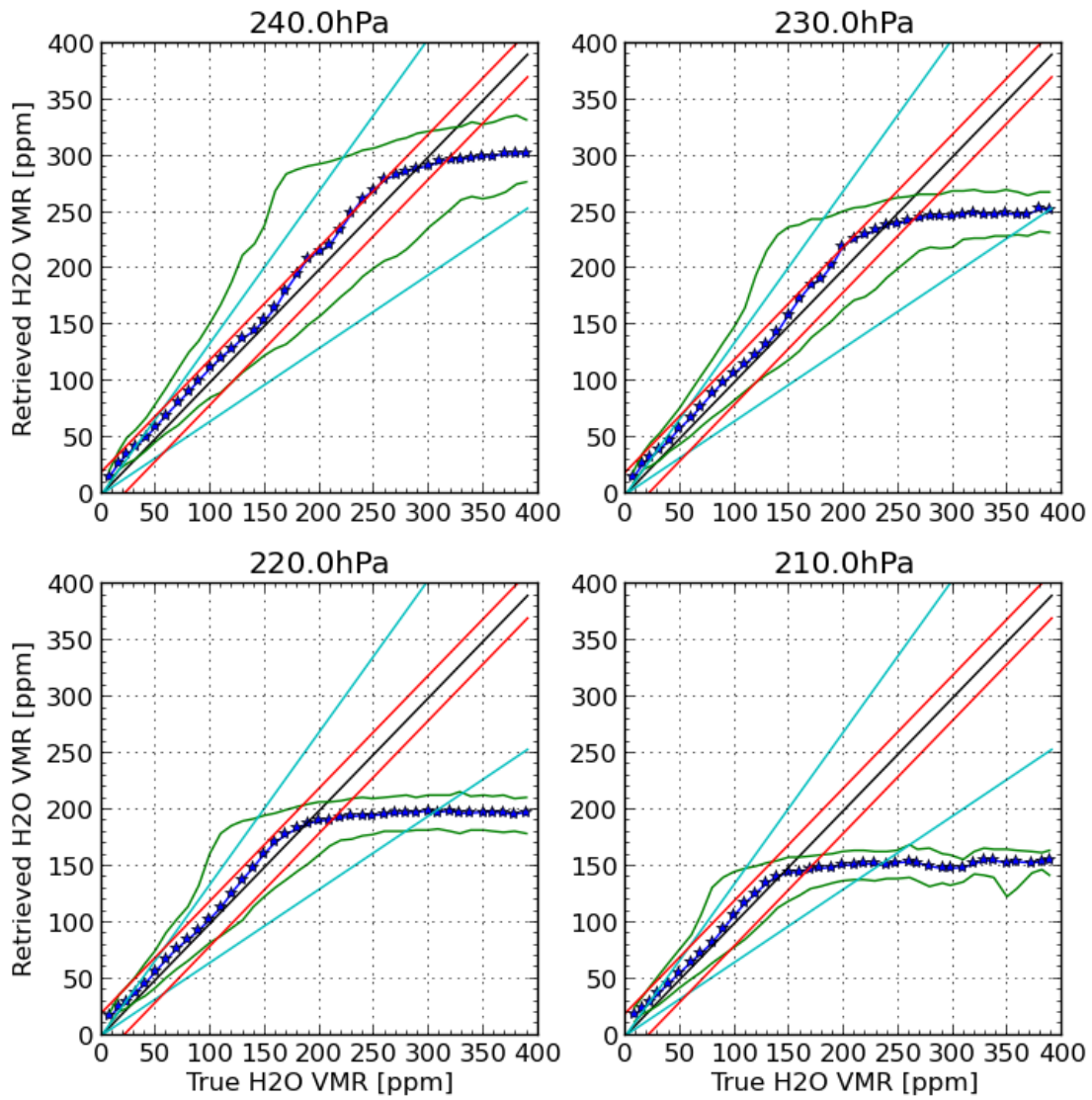


Figure 10. As Figure 6 but for H₂O volume mixing ratio at various pressure levels, and red lines represents a 20 ppm error, and cyan lines a 35 % error.

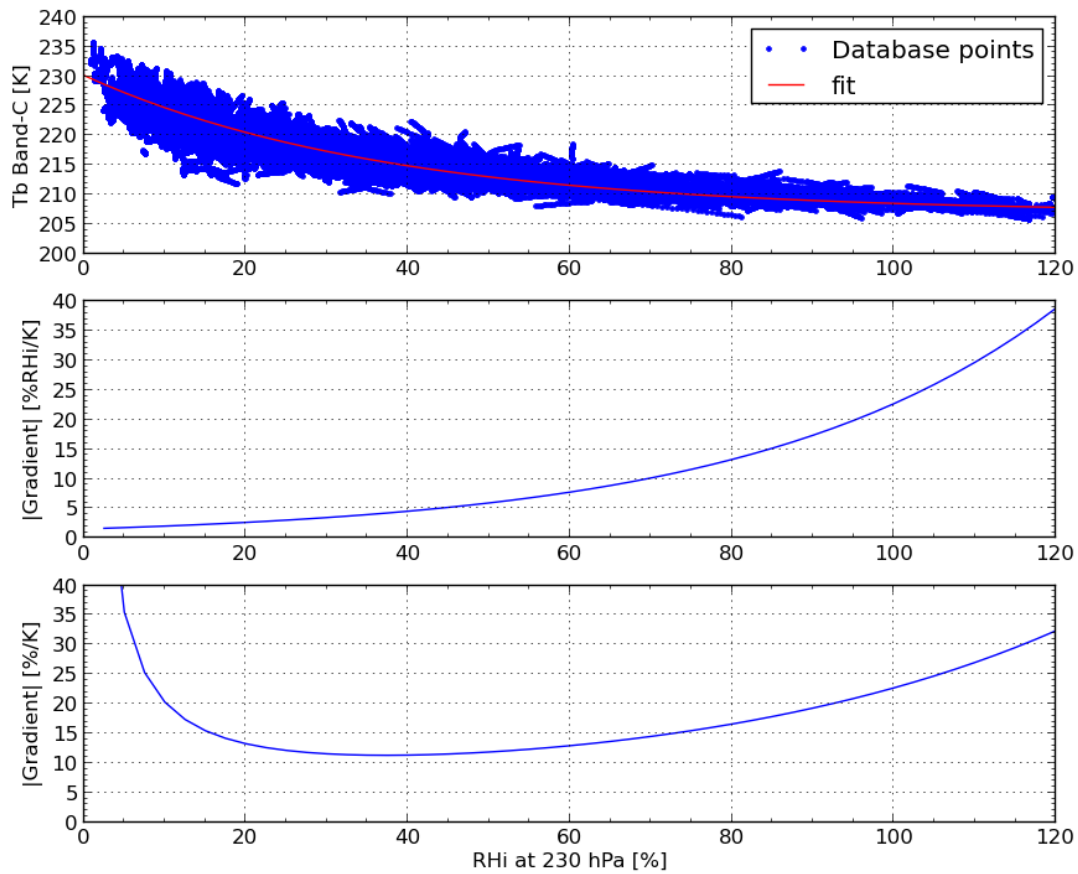


Figure 11. The upper panel shows a scatter-plot of Tb as function of RHi at 230 hPa for Band-C of clear sky retrieval database states. Only simulations from tangent heights between -10 to -5 km is shown. The red curve is a fit ($Tb=a+ b \times \exp(-c \times RHi)$) to the blue data-points. The middle and lower panel shows absolute value of the gradient in absolute and relative terms, respectively, as function of RHi for the fit in the upper panel.

Table 2. Estimated error from various sources for the relative humidity product (data is derived for RHi=70%).

Error source	perturbation	dTb	RHi error
Systematic errors			
Spectroscopic setup/ intensity calibration	see text for details	1 K	10% RHi or 14%
Tangent height	140 m	0.02 K	0.2% RHi or 0.3%
ECMWF temperature	1 K	•	2% RHi or 3%
a priori	•	•	5% RHi or 7 %
Root Sum Square , Systematic errors			11.4% RHi or 16.3%
Random errors			
Captured uncertainty	•	•	10% RHi or 14%

Figure 9 shows retrieved relative humidity w.r.t. ice (RHi) for four vertical layers. The retrieval precisions are best for the two middle layers, as for the cloud ice retrieval. Best performance, with a precision around 10% RHi in absolute terms or 16% in relative terms, is found for the layer between 250-200 hPa (finally the 260-200 hPa layer was chosen for the level2 product).

Retrieved RHi values are significantly underestimated for wet conditions. The reasons for this depends mainly on two facts. The first reason is that the measured signal saturates for high RHi (see Figure 10). The retrieval then tend to underestimate RHi for a wet atmosphere as the a priori gives that a drier atmosphere is a more likely solution. The second reason is due to that clouds and water vapor influences the measurements in a very similar way, and it is, in principle, impossible to separate between these two. The retrieval method applied uses a priori information for this purpose, and effectively, a very wet clear sky atmospheric state will be classified as a cloudy atmospheric state with a relative humidity around 100%.

Figure 10 shows retrieved H₂O volume mixing ratio (VMR) for four pressure levels (240,230,220, and 210 hPa). The retrieval precision is in the order of 35%. Retrieved H₂O vmr profiles are even more influenced by the a priori, than the relative humidity product. This is the case, as for clear-sky conditions the measured signal is more closely proportional to RHi than VMR. Therefore, the RHi product can be seen as the the main product within this project.

Figure 11 provides information that is used for assessing the accuracy of SMILES RHi observation. The upper panel of Figure 10 shows simulated clear sky Tb as function of RHi for Band-C. A non-linear relationships between Tb and RHi is clearly seen. The more wet the atmosphere is, the less is the measurement response for a change in RHi. The lower panels can be used for a simple estimation (neglecting the a priori information usage) of how a 1 K change in measured Tb will affect the retrieval. For example, at 70% RHi a 1 K change in Tb will change the retrieved RHi by around 10% RHi (At 120 % RHi this change is around 40% RHi).

In Table 2, an estimate of the accuracy of the RHi product is given. The accuracy depends on RHi for these observations. The accuracy (at least in absolute terms) is better for drier conditions than for more wet conditions. In Table 2, estimated accuracy for RHi around 70% is given. We treat systematic errors arising from spectroscopic setup and intensity calibration as one unit in the error budget, as they are so closely related for the retrieval methodology applied. In Section [Comparison of SMILES measurement with simulations](#) it was shown that the agreement between clear sky simulations and calibrated SMILES measurements is better than 1 K. A 1 K systematic error translates into an 10% RHi systematic error.

The a priori data has an impact of the retrieval. Thus, a systematic error in the a priori data will effect the accuracy of the retrieval. In fact, even perfect a priori data will introduce a systematic error, as retrieved state will be biased towards the a priori mean. Figure 8 shows that simulated retrieved RHi was underestimated by ~5% RHi for states with a RHi around 70% RHi. If the a priori distribution would have been uniformly distributed this would not have been the case. We therefore assign a 5% RHi systematic error due to the a priori usage. For averaged data this error can be reduced as described in [Rydberg²](#).

The total estimated systematic uncertainty is 11.4% RHi or 16.3% in relative terms, and the precision is 10% RHi or 14 % in relative terms.

4 The level2 products

Two different but similar sets of level2 products of upper tropospheric water have been processed. A first set of level2 product (the IWPRH product) includes upper tropospheric ice water path (IWP) and relative humidity (RH) and this can be seen as the main retrieval product within this project. A second set of level2 product (the H₂O product) includes water vapor in unit of volume mixing ratio (VMR).

All products are reported together with an uncertainty estimate. The estimated random errors includes effects of thermal noise, uncertainties due to instrument gain non-linearity, pointing error, uncertainty in atmospheric temperatures, and smoothing error (see further in Section [Retrieval characterization](#)).

The level2 files contain retrieval from measurements within the tropical region (30N to 30S). However, the retrieval method (including the a priori data) applied works best within the 20N to 20S region.

4.1 The IWPRH product

The two level2 products are ice water path (IWP) and relative humidity (RH). The IWP-product is the column ice mass above 260 hPa and has the unit of [g/m²]. The RH-product is the layer averaged relative humidity w.r.t. ice (RHi) between 260 and 200 hPa, and has the unit of [% RHi]. The RHi and IWP products have precisions of ~10% RHi and 70%, respectively (see section [Retrieval characterization](#)).

A level2-file is a collection of data from all scans of a single day from a unique band-combination. The level-2 files are named as, for example, SMILES_L2r_IWPRH-std008_CB_001_20100407.he5. This file contains retrieved IWP and RH data from the band-combination C and B from the date 2010-04-07.

Each file has the following structure:

HDFEOS

ADDITIONAL

FILE_ATTRIBUTES

L1BID: level1b identifier, 1-D array,64-bit integer

Index: index within level1b file identifier, 1-D array, 64-bit integer

SWATHS

IWP-std008

Data Fields

L2IWPValue: retrieved ice water path value, [g/m²], 1-D array, 64-bit floating-point

L2IWPPrecision: estimate of random retrieval error, [g/m²], 1-D array, 64-bit floating-point

Tangent_height: tangent height, [km], 1-D array, 64-bit floating-point

Pressure_tp: pressure grid, [hPa], 2-D array, 64-bit floating-point

Temperature_tp: ECMWF temperature profile, [K], 2-D array, 64-bit floating-point

Tb: Brightness temperature, [K], see section [Data quality and filtering recommendation](#), 2-D array, 64-bit floating-point

Quality: level1b quality, [-], see section [Data quality and filtering recommendation](#), 1-D array, 64-bit integer

Geolocation Fields

Latitude: latitude at 10 km height along line of sight [-30,30], [degree], 1-D array, 64-bit floating-point

Longitude: longitude at 10 km height along line of sight [-180,180], [degree], 1-D array, 64-bit floating-point

TimeUTC: measurement timestamp, 1-D array,String length = 19 (eg. 2009-10-14T00:07:46)

Altitude_tp: Approximate altitude at Latitude, Longitude, Pressure_tp, [m], 2-D array, 64-bit floating-point

RH-std008

Data Fields

L2RHvalue: retrieved relative humidity value, [% RHi], 1-D array, 64-bit floating-point

L2RHPrecision: estimate of random retrieval error, [% RHi], 1-D array, 64-bit floating-point

Geolocation Fields

same as for IWP-std008

4.2 The H2O product

The H2O product contains retrieved upper tropospheric water vapor in unit of volume mixing ratio (VMR). For the considered measurements and for clear sky conditions the measurements have mainly sensitivity to water vapor in the atmospheric layer between 260 to 200 hPa. Water vapor VMR profiles are retrieved on a fine pressure grid ranging from 280 to 180 hPa with a grid spacing of 10 hPa, which clearly is much finer than the vertical resolution of the measurements. However, the VMR estimate for each pressure level represent a best estimate for that specific level, with a vertical resolution of a few kilometers. The H2O product has a precision of about 35% (see section [Retrieval characterization](#)).

The level2 file structure is described below:

HDFEOS

ADDITIONAL

FILE_ATTRIBUTES

L1BID: level1b identifier, 1-D array, 64-bit integer

Index: index within level1b file identifier, 1-D array, 64-bit integer

SWATHS

H2O-std008

Data Fields

L2H2Ovalue: retrieved VMR water vapor profile, [ppm], 2-D array, 64-bit floating-point

L2H2OPrecision: estimate of random retrieval error, [ppm], 2-D array, 64-bit floating-point

Tangent_height: tangent height, [km], 1-D array, 64-bit floating-point

Pressure_tp: pressure grid, [hPa], 2-D array, 64-bit floating-point

Temperature_tp: ECMWF temperature profile, [K], 2-D array, 64-bit floating-point

Tb: Brightness temperature, [K], see section [Data quality and filtering recommendation](#), 2-D array, 64-bit floating-point

Quality: level1b quality, [-], see section [Data quality and filtering recommendation](#), 1-D array, 64-bit integer

Geolocation Fields

Latitude: latitude at 10 km height along line of sight [-30,30], [degree], 1-D array, 64-bit floating-point

Longitude: longitude at 10 km height along line of sight [-180,180], [degree], 1-D array, 64-bit floating-point

TimeUTC: measurement timestamp, 1-D array, String length = 19 (eg. 2009-10-14T00:07:46)

Altitude_tp: Approximate altitude at Latitude, Longitude, Pressure_tp, [m], 2-D array, 64-bit floating-point

4.3 Data quality and filtering recommendation

The level2 files contain a Quality field, and the quality value is determined from level1b data for each inverted measurement.

The quality value can be 0,1,10,11,100,110, or 111, and the recommended usage is to only consider level2 data that has quality 0 or 10.

The quality status is determined from three points (and only from L1b-data):

1. Tb and Tsys values are unrealistic (quality+=1) (see Figure 12 to 14)
2. Attitude data can be problematic (quality+=10)
3. Solar panel can be in the line of sight (quality+=100)

The Tb and Tsys quality check are based on Tbs of the measured bands, Tsys, and Tb around the strong ozone transition at 625.37 GHz, covered by both band A and B. The quality filter is developed to identify data points that lie outside (are unrealistic) the cluster of data points.

Data-points are accepted if Tb around the O3-line lies in the range 160 to 230 K. A close to linear relationships (with a +/-10 K scatter) is found between Tb of Band-A (or Band-B) and Tb around the O3-line, for the majority of data-points. Data-points found outside 20 K of the "linear relationship" is rejected, and a possible cause to these data-points are pointing errors.

Figures 12 to 14 show the result of applying the quality (step 1 above) filter on the data-set. The red points have quality 1, and are considered to be data points with unrealistic values (not perfect calibrated).

The level1b data that is used to determine the Quality field is contained within the Tb field of the level2 file. The Tb field has 8 rows (for one measurement). It is here explained what these values are (if the measurements are from band A and B). Index 1 and 2 are Tb from band A and B, respectively. Index 3 and 4 are Tsys from band A and B, respectively. Index 5 and 6 are Tb around the strong ozone line for band A and B, respectively. Index 7 and 8 are FlagSTT and FlagANT, respectively. If the measurements are from band C and A, or band C and B, index 1 is Tb from band C and index 2 is Tb from band A or B, and so on.

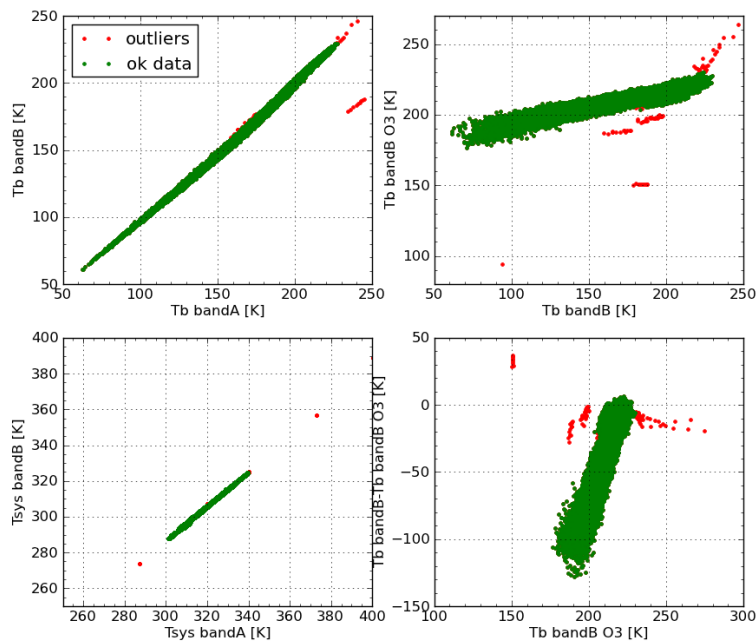


Figure 12. The upper left panel shows Tb from band A vs. Tb from band B. The upper right panel shows Tb from band B vs. the Tb around the strong (almost optically thick) ozone line around 625.37 GHz. The lower left panel shows Tsys from band A vs. band B. The lower right panel shows Tb from band B vs. the difference in Tb from band B and around the ozone line.

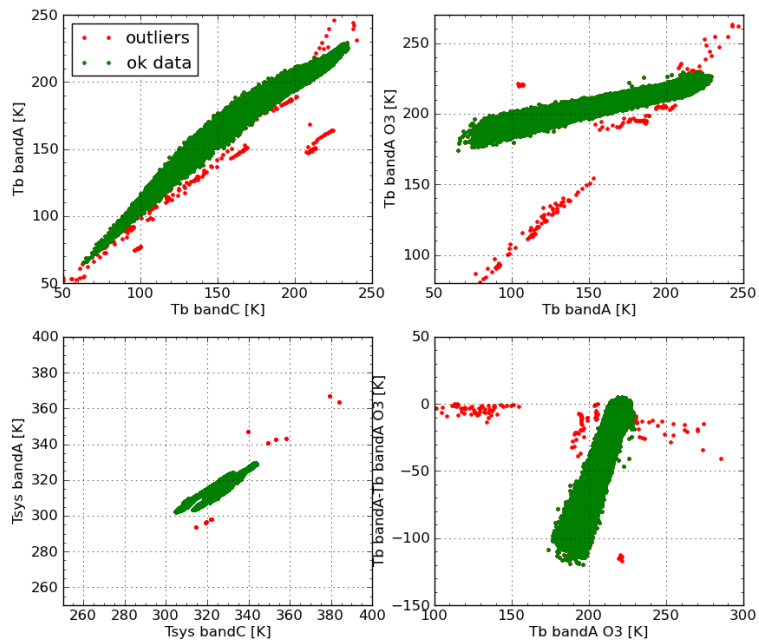


Figure 13. As Figure 12 but for band C and A.

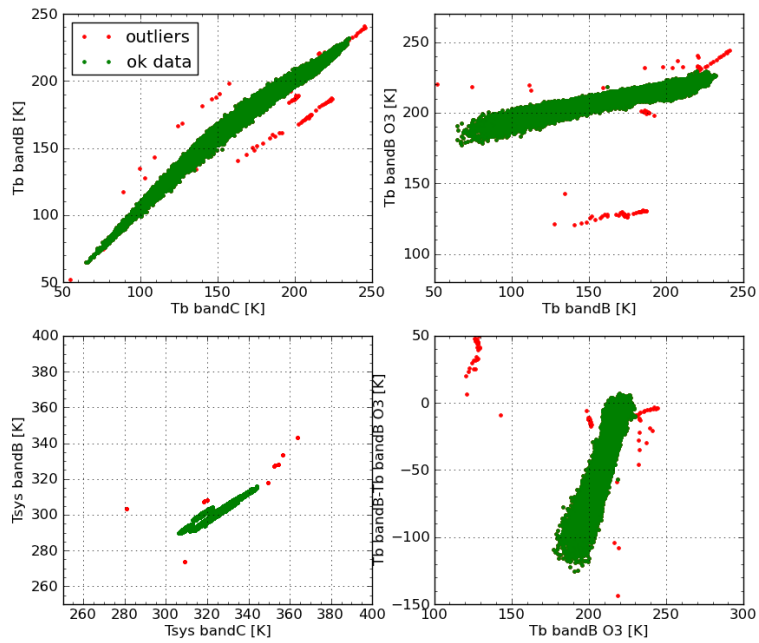


Figure 14. As Figure 12 but for band C and B.

4.4 Example results

Figure 15 shows averaged fields of the two products of the IWPRH (section [The IWPRH product](#)) data-set. The geographical structure is pure measurement information as the same a priori is used for the complete tropical region.

Figure 16 shows diurnal variation of the two products for five selected regions. Most clear diurnal variation can be seen in the IWP product. Over the tropical land regions the daily maxima occur during the afternoon and over the tropical ocean regions the daily maxima occur during the night or morning.

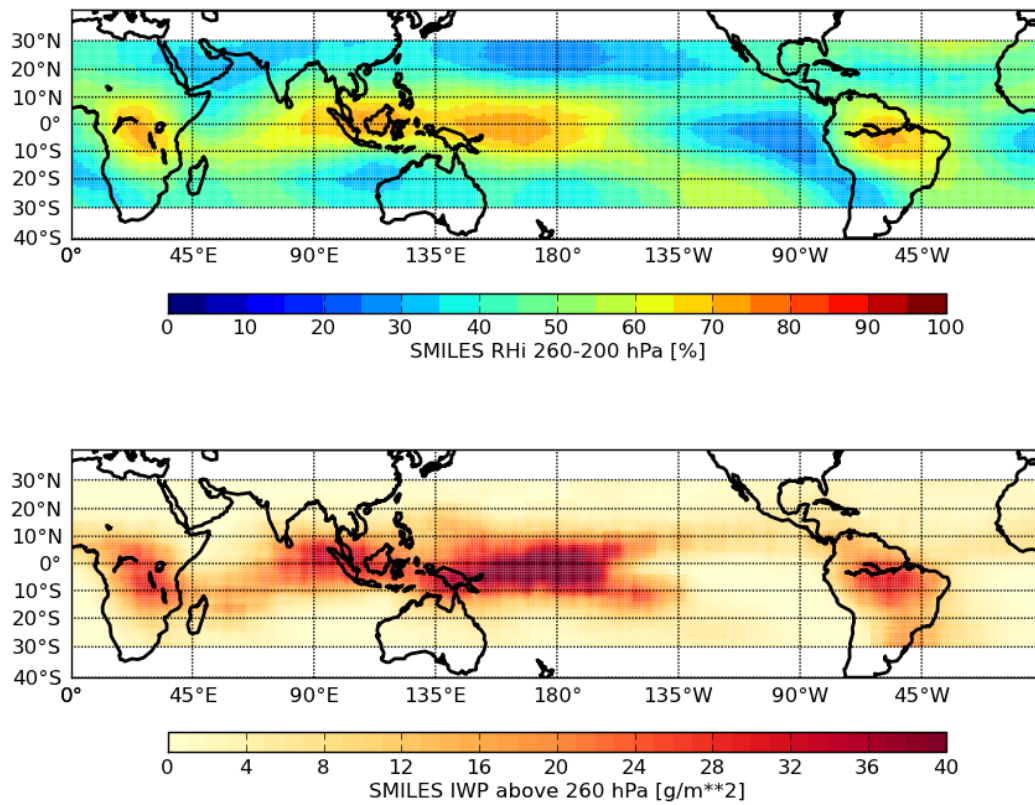


Figure 15. The upper panel shows retrieved averaged RH field for the complete data-set. The lower panel shows retrieved averaged IWP field for the complete data-set.

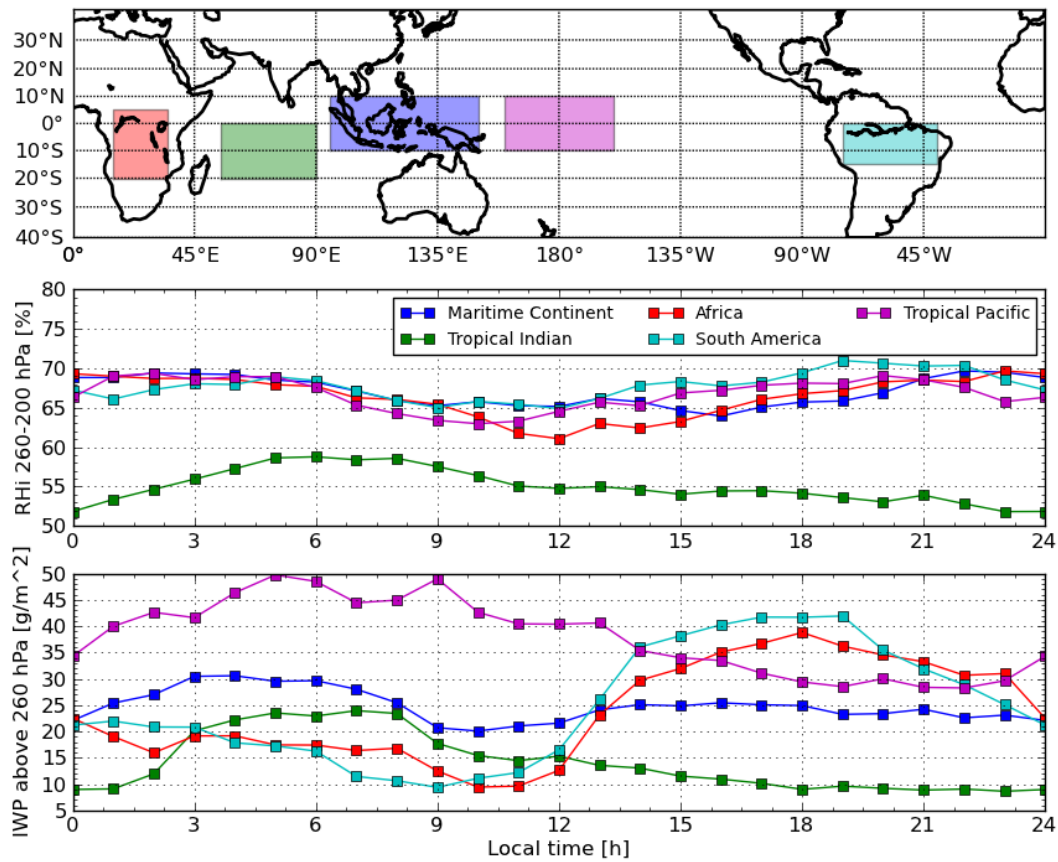


Figure 16. Retrieved diurnal variations of RH (middle panel) and IWP (lower panel) for the regions defined in the upper panel panel. Each data point is averaged over ± 3 hours.

<http://onlinelibrary.wiley.com/doi/10.1029/2010JD014379/abstract;jsessionid=790E9C152F56CF150391D7857A8142C0>
 2(1, 2, 3, 4) <http://www.atmos-meas-tech.net/2/621/2009/amt-2-621-2009.html>
 3 <http://www.atmos-chem-phys.net/10/11519/2010/acp-10-11519-2010.html>
 4(1, 2, 3, 4) <http://ieeexplore.ieee.org/xpl/articleDetails.jsp?arnumber=6423279>
 5 <http://www.sat.ltu.se/arts/>
<http://journals.ametsoc.org/doi/abs/10.1175/1520-0469%281997%29054%3C2187%3APOTCIC%3E2.0.CO%3B2>